Amplitude measurement of weak sinusoidal water surface acoustic wave using laser interferometer

Lieshan Zhang (张烈山)*, Xiaolin Zhang (张晓琳), and Wenyan Tang (唐文彦)**

School of Electrical Engineering and Automation, Harbin Institute of Technology, Harbin 150001, China
**Corresponding author: zhanglieshan@163.com; **corresponding author: zhangxiaolin@hit.edu.cn*
Received April 28, 2015; accepted July 9, 2015; posted online August 5, 2015

To determine the amplitude of weak sinusoidal water surface acoustic wave (WSAW), a method based on the spectrum analysis of the phase-modulated interference signal is developed. Calculated from the amplitude spectrum of the detection signal, a characteristic ratio indicates that the phase-modulation depth of a WSAW is suggested by determining the amplitude of a WSAW according to their functional relationship. Experimental investigations for a 4 kHz WSAW evaluate the measurement's precision with an amplitude measurement standard deviation of 0.12 nm. The measurement accuracy also is demonstrated by the experimental investigations. The theory of this method is briefly described, and the experimental setup is presented.
OCIS codes: 120.3180, 120.7280, 060.2370, 010.7340.
doi: 10.3788/COL201513.091202.

Caused by the underwater acoustic pressure field, the water surface acoustic wave (WSAW) is regarded as a kind of Rayleigh wave that propagates along the air-water interface. Generally, it has a very weak amplitude, with a scale of several nanometers. As a result of the acoustic impedance mismatch, which occurs when the wave is incident on the air-water boundary, the acoustic pressure in the water causes the surface to vibrate at the frequency of the acoustic pressure, and a WASW appears. Hence, a WSAW carries some of the information of the underwater sound field. WSAW detection to obtain underwater acoustic signals has gradually become a new research field in ocean engineering[1–8]. Obviously, the determination of a WSAW's amplitude is of great interest and could be utilized in many applications, as it is a very crucial parameter in assessing the sound intensity and localization of an underwater sound source. Also, a WSAW is usually drowned in large-amplitude surface vibrations caused by environmental perturbations, and it is quite difficult to measure it accurately.

A laser interferometer was previously used in the detection of solid surface waves. It has been introduced as a kind of industry standard for calibrating vibration sensors[9,10]. In order to detect a WSAW and underwater acoustic signals, it was used by Antonelli and Kirsteins[11], Blackmon *et al.*[12], and Zhang[13,14] *et al.* to observe water surface waves. Interferometric techniques using coherent laser radiation to measure the acoustic signals on a vibrating surface have been successfully put into effect; the researchers[2,3] reported that WSAWs can be detected by a laser interferometer from a randomly moving water surface. At present, the laser interferometer is mainly used to determine the frequency of a WSAW with an uncertainty of 1.5 Hz. In addition, WSAWs can be regarded as a reflex-type sinusoidal phase grating, and amplitude of a WSAW can be calculated using the geometric parameters of the diffraction pattern received by a CCD[15]. The amplitude of a WSAW can be determined by means of optical diffraction, but this has several limitations: it never works when the frequency of a WSAW is larger than 100 Hz, or if any environmental perturbation appears on the water's surface. Phase variation caused by a WSAW can be extracted from the demodulated results of the interferometric signal. The maximum phase variation in the interferometer detection signal can be caused by a WSAW and can be less than 0.02 rad. As such, the phase demodulation method based on the interferometer also does not work well in the presence of environmental perturbations.

In this Letter, we discussed the amplitude-frequency distribution features of WSAW detection signals. As opposed to the previous methods, we proposed an algorithm to determine the amplitude of a WSAW that based on the frequency spectrum analysis of the interference signal. The effects of the phase modulation by the WSAW can be observed in the amplitude spectrum of the interference signal, and a characteristic ratio indicates that the modulation depth was suggested in calculating the amplitude of the WSAW according to their certain functional relationship. The performance of the proposed method was examined by means of computer simulation and verified by the experimental investigations. In the laboratory, the amplitude measurement precision was evaluated by multiple amplitude measurements for a 4 kHz WSAW with a standard deviation of 0.12 nm. The accuracy of this method was verified by the comparisons between the experimental results and the theoretical analysis of the WSAW.

We imagine that the vibrations on the water's surface can be divided into two parts: the low-frequency environmental perturbation with a large amplitude (in the laboratory, the amplitude of the environmental perturbation on the water's surface can be larger than 20 μm), and the microwave, which is known as the WSAW. The water's surface is probed by the laser interferometer to detect

the composite vibrations. According to the principle of the Doppler interferometer[16,17], when filtered by the DC component, the interference signal detected by a photo detector can be described as

$$P(\mathrm{t}) = A_\mathrm{d}\cos\{2k[A_\mathrm{n}\sin(\omega_\mathrm{n}t+\varphi_\mathrm{n})+A_\mathrm{s}\sin(\omega_\mathrm{s}t+\varphi_\mathrm{s})]+\varphi\}, \tag{1}$$

where A_d is the gain factor corresponding to the optical amplitudes of the two laser beams and the amplifier of the data acquisition module, k is the wavenumber of the coherent laser. A_n, ω_n, and φ_n respectively denote the amplitude and the angular frequency or the phase of the environmental wave; similarly, A_s, ω_s, and φ_s denote the amplitude, the angular frequency, and the phase of the WSAW. t denotes time, and φ denotes the initial phase, which is caused by the nominal optical path difference between the two arms of the interferometer.

Equation (1) can be decomposed into a large number of components with different angular frequencies using the formulas of the trigonometric function and Bessel's equation

$$\exp[\mathrm{j}\beta\sin(\Phi)] = \sum_{n=-\infty}^{\infty}\mathrm{J}_n(\beta)\exp(\mathrm{j}n\Phi). \tag{2}$$

Let $\mathrm{A}(\omega)$ represent the amplitude of the component with the angular frequency ω. According to the decomposed result of Eq. (1), the amplitudes of components with angular frequencies of $(2m+1)\omega_\mathrm{n}$, $2m\omega_\mathrm{n}$, $(2m+1)\omega_\mathrm{n}+\omega_\mathrm{s}$, and $2m\omega_\mathrm{n}+\omega_\mathrm{s}$ can be expressed as

$$\begin{cases} A[(2m+1)\omega_\mathrm{n}] = A_\mathrm{d}\sin(\varphi)\mathrm{J}_0(2kA_\mathrm{s})\mathrm{J}_{2m+1}(2kA_\mathrm{n}) \\ A(2m\omega_\mathrm{n}) = A_\mathrm{d}\cos(\varphi)\mathrm{J}_0(2kA_\mathrm{s})\mathrm{J}_{2m}(2kA_\mathrm{n}) \\ A[(2m+1)\omega_\mathrm{n}+\omega_\mathrm{s}] = A_\mathrm{d}\cos(\varphi)\mathrm{J}_1(2kA_\mathrm{s})\mathrm{J}_{2m+1}(2kA_\mathrm{n}) \\ A(2m\omega_\mathrm{n}+\omega_\mathrm{s}) = A_\mathrm{d}\sin(\varphi)\mathrm{J}_1(2kA_\mathrm{s})\mathrm{J}_{2m}(2kA_\mathrm{n}) \end{cases}. \tag{3}$$

where m is an integer.

Then, we define the characteristic ratio R as

$$R = \sqrt{\frac{\sum_m A[(2m+1)\omega_\mathrm{n}]}{\sum_m A[(2m+1)\omega_\mathrm{n}+\omega_\mathrm{s}]}\frac{\sum_m A(2m\omega_\mathrm{n})}{\sum_m A(2m\omega_\mathrm{n}+\omega_\mathrm{s})}} = \frac{\mathrm{J}_0(2kA_\mathrm{s})}{\mathrm{J}_1(2kA_\mathrm{s})}, \tag{4}$$

where $2kA_\mathrm{s}$ is the phase modulation depth caused by the WSAW. Therefore, R is a function of A_s, and also there is an inverse function of $R(A_\mathrm{s})$ when the value of A_s is in a certain interval. Based on the above, we can determine the value of A_s by the value of R. Due to the properties of Bessel functions of the first kind, we can draw the conclusion that when A_n approaches infinity, ratio R can be rewritten as

$$R|_{A_\mathrm{n}\to\infty} = \frac{\sum_m A(m\omega_\mathrm{n})}{\sum_m A(m\omega_\mathrm{n}+\omega_\mathrm{s})}. \tag{5}$$

The nominal optical path difference between the two arms of the interferometer seems very difficuly to determine. Compared with the WSAW, the amplitude of water surface's environmental wave is a particularly large value; therefore, we can ignore the effect of initial phase φ and calculate the characteristic ratio R using Eq. (5) to take the place of Eq. (4). The numerical simulation results show that the amplitude calculation error caused by ignoring φ is smaller than 0.05 nm.

Actually, there may be various components in the environmental perturbations. Assuming that there are several environmental perturbations with different frequencies and amplitudes on the water's surface, let ω_i and A_i denote the angular frequency and the amplitude of one environmental perturbation, as well as ω_j and A_j. Ignoring the initial phase φ and the gain coefficient A_d, let A_1 represent the amplitude of the spectrum component at a frequency of $\mathrm{a}\omega_\mathrm{i}+\mathrm{b}\omega_\mathrm{j}$. Then, A_1 can be written as

$$A_1 = \mathrm{J}_0(2kA_\mathrm{s})\mathrm{J}_\mathrm{a}(2kA_\mathrm{i})\mathrm{J}_\mathrm{b}(2kA_\mathrm{j})\prod_{\substack{m=1,\\ m\neq\mathrm{i,j}}}^{N}\mathrm{J}_0(2kA_m), \tag{6}$$

where N denotes the component number of the environmental perturbations. Similarly, let A_2 represent the amplitude of the component at a frequency of $\mathrm{a}\omega_\mathrm{i}+\mathrm{b}\omega_\mathrm{j}+\omega_\mathrm{s}$. Then, A_2 can be written as

$$A_2 = \mathrm{J}_1(2kA_\mathrm{s})\mathrm{J}_\mathrm{a}(2kA_\mathrm{i})\mathrm{J}_\mathrm{b}(2kA_\mathrm{j})\prod_{\substack{m=1,\\ m\neq\mathrm{i,j}}}^{N}\mathrm{J}_0(2kA_m). \tag{7}$$

Obviously, the ratio of A_2 and A_1 is equal to the defined characteristic ratio R, and so is the amplitude ratio of any couple of components with a certain frequency difference of ω_s. As a result, in the frequency domain in which the signal spectrum band caused by the WSAW could be clearly distinguished from the spectrum band caused by environmental perturbations, the phase modulation depth of the WSAW, $2kA_\mathrm{s}$, can be determined according to the amplitude-frequency distribution of the detection signal.

In order to decline the random error in the calculation of R and eliminate the effect of initial phase φ, we use amplitude sums S_1 and S_2 to calculate ratio R: S_1 denotes the amplitude sum of the components in the low-frequency spectrum band, and S_2 denotes the amplitude sum of the components with frequency shift of ω_s. This could significantly improve the calculation repeatability of R. Also, let ω_a denote the frequency resolution of the data acquisition module, so assuming that the width of the low-frequency band caused by the environmental perturbations is equal to $N\omega_\mathrm{a}$, then the calculation formulas of S_1, S_2, and R can be described as

$$\begin{cases} S_1 = \sum_{i=1}^{N} A(i\omega_a) \\ S_2 = \sum_{i=1}^{N} A\left[\left(\frac{\omega_s}{\omega_a} + i\right)\omega_a\right] \\ R = \frac{S_1}{S_2} = \frac{J_0(2kA_s)}{J_1(2kA_s)} \end{cases}. \quad (8)$$

Presupposing that the frequency of the WSAW, ω_s, is known, and by converting the detection signal to the frequency domain using the Fourier transform, we can calculate the values of R and A_s according to Eq. (8) and the amplitude spectrum of the detection signal. Figure 1 illustrates the relationship between R and A_s, when A_s is in the interval of 0.5–25 nm, and the wavelength of the laser is set to 1064 nm as an example. The analytical solution of the inverse function of $R(A_s)$ is of great difficulty to obtain. We can determine the value of A_s by using a reference table.

Generally, we use a Fast Fourier Transform algorithm to obtain the amplitude spectrum of the detection signal. Since the Fourier transform is a kind of linear transform, the waves in any subinterval of observation time can be detected in the final transform results, and the characteristic ratio can be calculated accurately even if the environmental perturbations in the phase of the interference signal usually randomly emerge in the time domain, i.e., some components maybe only last for a short subinterval. The Fourier spectrum of a simulated signal is shown in Fig. 2. The observation time is 1 s, and the frequency resolution is 1 Hz. In the different subintervals, the environmental perturbations in the phase of the detection signal consist of two or three components with distinct frequencies and amplitudes. The amplitude of the WSAW was set to 10 nm, and its frequency was 2 kHz.

After calculating the characteristic ratio and amplitude of the WSAW using Eq. (8) and using the Fourier transform results of the simulated signal, we can calculate that the length of the low-frequency spectrum band is about 800 frequency resolutions. The value of S_1 is 11.3926 and S_2 is 1.1424, and the ratio between them is 9.9725. Then, we can determine the amplitude of the WSAW using the reference table. The calculated amplitude of the WSAW is 10.05 nm, which is in sufficient agreement with the set value despite a tiny error of 0.05 nm.

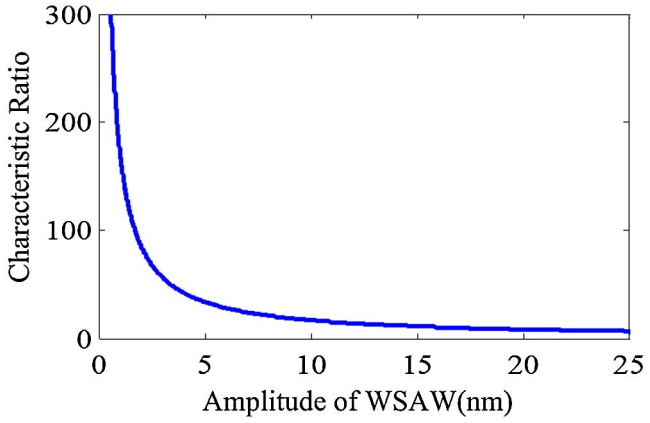

Fig. 1. Relationship curve of characteristic ratio to amplitude of WSAW (A_s is in the interval of 0.5—25 nm).

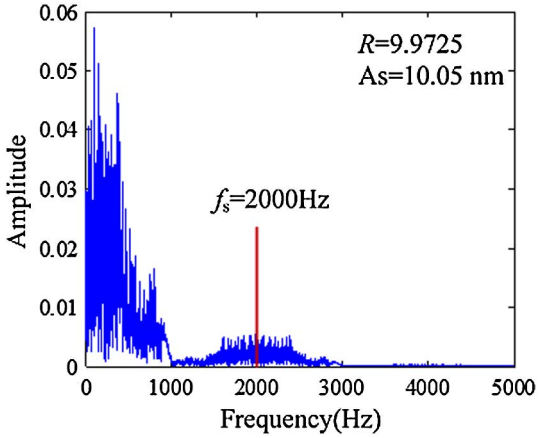

Fig. 2. Fourier spectrum of the simulated interference signal.

The accuracy of this method was experimentally confirmed with the setup depicted in Fig. 3. A sinusoidal voltage, which was sent by a signal generator, was applied to drive an acoustic transmitter (e.g., an underwater loudspeaker) to produce a sound field and excite the WSAW. A typical Michelson interferometer consists of a coherent laser at a wavelength of 1064 nm, fiber couplers, a circulator, a collimator, and the like. A large-diameter collimator can be used to send the interrogating laser beam to the water's surface, and in the meantime, it also can collect the phase-modulated reflected beam. A photo detector converts the optical interference signals into electrical signals.

Letting signal generator output a standard sinusoidal signal at a frequency of 4 kHz, after power amplification, the sinusoidal signal drove the acoustic transmitter to excite a sinusoidal WSAW. The sound pressure level (SPL) of the underwater acoustic radiation was about 101 dB re 20 μPa, and the acoustic transmitter was placed at a depth

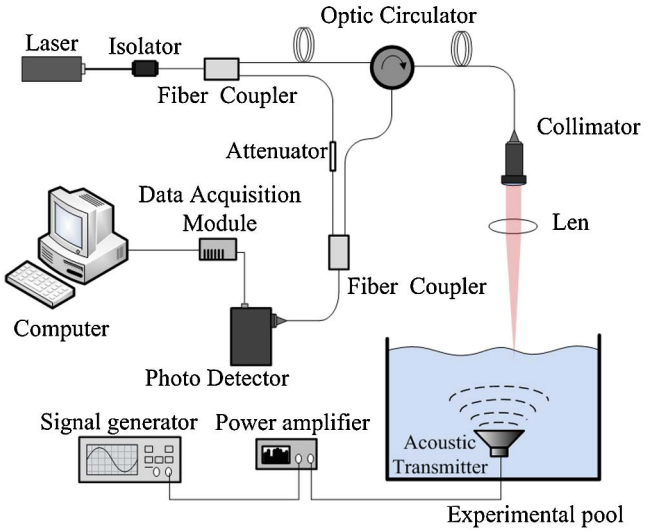

Fig. 3. Laboratory setup for amplitude measurement of WSAW.

of about 500 mm. By probing the water's surface using interferometer shown in Fig. 3, we acquired a interference signal and filtered the DC component. Its time-domain waveform and Fourier spectrum are depicted in Fig. 4. The sampling rate of the data is 51200 samples per second and the number of data samples is 51200, so the frequency resolution is equal to 1 Hz.

Several groups of amplitude measurement experiments for a 4 kHz sinusoidal WSAW were conducted to examine the precision of this method. According to the Fourier spectrum of the experimental signals, the width of the low-frequency spectrum band caused by environmental perturbations is about 500 frequency resolutions, and we can calculate the characteristic ratio and the amplitude of the WSAW by using a Fourier transform and Eq. (8). The calculation results are given in Table 1. The standard deviation of ratio R is 0.8050, and the deviation of the amplitude is 0.1179 nm. The experimental results confirmed the measurement precision of the proposed method. Moreover, from Eq. (8) and Fig. 1, we can infer that when A_s becomes bigger, the repeatability of ratio R gets smaller, so that the measurement precision of amplitude A_s can be maintained in a certain interval.

It is impossible to obtain the true value of the WSAW's amplitude, but in order to investigate the correctness of the measurement results (i.e., in order to investigate the accuracy of this method), amplitude measuring experiments for WSAWs with different frequencies and different sound levels were carried out. According to the acoustic theory[18,19], the amplitude of a WSAW is proportional to the incident sound pressure, and it can be inversely proportional to its frequency. Adjusting the driving voltage of the signal generator and the gain of the amplifier makes the acoustic transmitter keep the SPL of the acoustic radiation at about 80, 85, 90 and 95 dB. The transmitter was placed at a depth of about 500 mm. From observing the experimental results of the amplitude measurements of the WSAWs with different frequencies, as shown in Fig. 5, we can draw a conclusion that as the frequency increasing, the amplitude of the WSAW becomes smaller. The amplitude of the WSAW is inversely proportional to the frequency, coinciding with the theoretical analysis of the WSAW.

Amplitude measuring experiments for WSAWs caused by different incident pressure sounds were also conducted. We can have the WSAWs maintain a stationary frequency of 1, 2, 3 and 4 kHz, while changing the SPL of underwater sound from 60 to 110 dB. Figure 6 shows the experimental results of the amplitude measurements for WSAWs at different incident sound intensities. From Fig. 6, we can observe that the amplitude of the WSAW becomes bigger as the incident sound level increases; thus, we can conclude that the amplitude of a WSAW is proportional to the intensity of the incident sound. These are two kinds of

Table 1. Calculation Results of Ratio R and Amplitude A_s for 4 kHz WSAW

No.	Characteristic Ratio R	Amplitude of WSAW A_s(nm)
1	36.0653	4.6933
2	35.3655	4.7865
3	33.7459	5.0158
4	34.8696	4.8549
5	34.7333	4.8727
6	34.6924	4.8778
7	34.9002	4.8499
8	35.3265	4.7915
9	33.5596	5.0701
10	35.8357	4.7238
σ	0.8050	0.1179

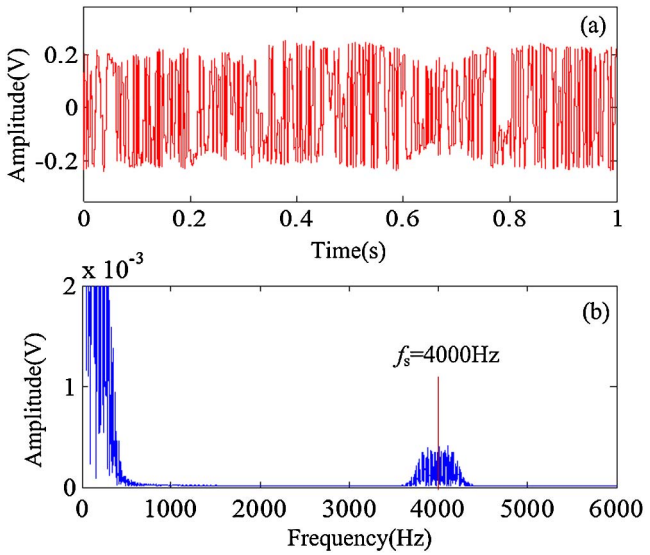

Fig. 4. Schematic of (a) time-domain waveform (the DC component was filtered) and (b) Fourier spectrum of experimental detection signal for 4 kHz WSAW.

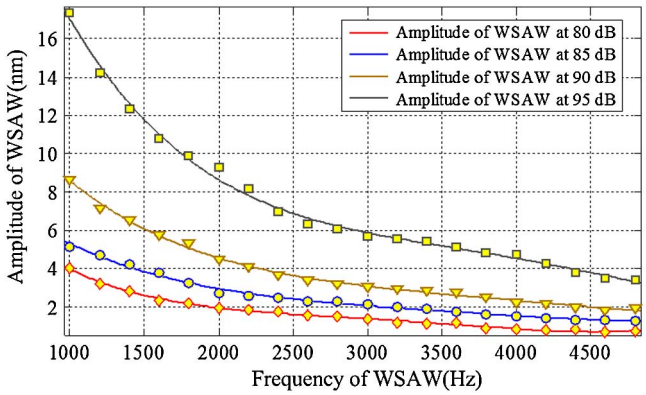

Fig. 5. Experimental results of amplitude measurements for WSAWs with different frequencies. SPL of underwater sound was kept at 80, 85, 90 and 95 dB.

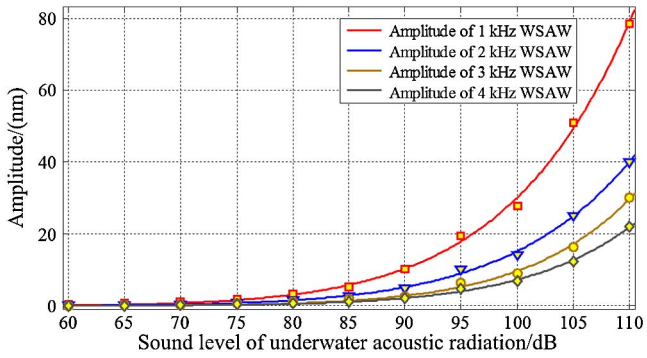

Fig. 6. Experimental results of amplitude measurements for WSAWs caused by different incident sound pressures. Frequencies of WSAWs were kept at 1, 2, 3 and 4 kHz.

amplitude measuring experiments that have effectively demonstrated the accuracy of the proposed amplitude measuring method.

In addition, this method performs two great properties in application: the frequency error tolerance and anti-noise performance. From Eq. (8), by using this method to determine the amplitude of the WSAW, we must first obtain the value of the frequency. Generally, the frequency of a WSAW is acquired by the measurement with an error of one frequency resolution (usually 1.5 Hz)[20]. This appears to be an error when calculating the value of S_2. Since S_2 is a cumulative value, we can almost ignore the influence of one resolution error in the frequency. Taking one group of 4 kHz WSAW experimental data for example, the value of amplitude A_s when calculated without the frequency error is 4.86 nm, and A_s calculated with a frequency error of 2 Hz is 4.83 nm. A_s calculated with a frequency error of −2 Hz is 4.90 nm, so the deviation is smaller than 0.05 nm. Thus, it can absolutely be ignored. Because of the statistical characteristics of Gaussian noise, we can easily eliminate its influence when calculating S_1 and S_2 by the spectrum analysis of the noise in the signal. In order to improve the accuracy of the amplitude determinations, it is best to deduct an estimate correction term corresponding with the noise spectrum from S_1 and S_2 when the interference signal has a low signal-to-noise ratio. However, there is also a limitation on the amplitude of the environmental perturbations when we apply this method. Several factors can influence how strong environmental perturbations can be tolerated by the proposed method, such as the wavelength of the coherent laser, the frequency of the environmental perturbations, the frequency of the WSAW, and the modulation depth of the WSAW. When the phase of the interference signal is deeply and well-modulated by a high-frequency WSAW, the proposed method can tolerate millimeter-scale environmental perturbations.

In conclusion, we propose a method to determine the amplitude of a weak sinusoidal WSAW that is based on the determination of a characteristic ratio and the Fourier spectrum analysis of the interference signal. The performance of this method is examined by the means of a computer simulation and verified by the experimental investigations. We observe and study the measurement precision and the accuracy of the proposed method. The amplitude measuring experiments of a WSAW with a frequency of 4 kHz are conducted to evaluate the measurement precision, with a standard deviation of 0.12 nm. Amplitude measuring experiments for WSAWs with different frequencies and sound levels are also carried out. The accuracy of this method is verified by the comparisons of the experimental results and the theoretical analysis of the WSAW. Furthermore, we discuss two great properties of the proposed method.

This work was supported by the National Natural Science Foundation of China under Grant No. 61108073.

References

1. M. S. Lee, B. S. Bourgeois, S. T. Hsieh, A. B. Martinez, L. Hsu, and G. D. Hickman, in *Proceedings of IEEE Southeastcon* 253 (1988).
2. L. Antonelli and F. Blackmon, J. Acoust. Soc. Am. **116**, 3393 (2004).
3. D. Farrant, J. Burke, L. Dickinson, P. Fairman, and J. Wendoloski, in *Proceedings of OCEANS'10 IEEE Sydney* (2010).
4. F. Blackmon and L. Antonelli, Proc. SPIE **5778**, 800 (2005).
5. A. R. Harland, J. N. Petzing, J. R. Tyrer, C. J. Bickley, S. P. Robinson, and R. C. Preston, J. Sound Vib. **265**, 627 (2003).
6. J. Wojtanowski, Z. Mierczyk, and M. Zygmunt, Proc. SPIE **7105**, 71050F (2008).
7. C. Zhou, K. Liu, J. He, J. Sun, R. Hang, G. Chui, R. Li, T. Yun, J. He, G. Shang, and Z. Tian, Proc. SPIE **3558**, 515 (1998).
8. T.-H. Zhou and N. He, in *Proceedings of 7th International Symposium on Antennas, Propagation and EM Theory* 617 (2006).
9. C. Li, Z. Huang, and X. Sun, Chin. Opt. Lett. **11**, S21201 (2013).
10. Y. Tan, Z. Zeng, S. Zhang, P. Zhang, and H. Chen, Chin. Opt. Lett. **11**, 102601 (2013).
11. L. T. Antonelli and I. P. Kirsteins, in *Proceedings of Oceans Conference Record (IEEE)* 999 (2000).
12. F. Blackmon, L. Estes, and G. Fain, App. Opt. **44**, 3833 (2005).
13. X. L. Zhang, W. Y. Tang, and H. P. Duan, in *Proceedings of 8th International Symposium on Test and Measurement* 1187 (2009).
14. X.-L. Zhang, W.-Y. Tang, and H.-Y. Sun, Opt. Precision Eng. **18**, 809 (2010).
15. R. Miao, X. Zhao, and J. Shi, Chin. J. Lasers **31**, 752 (2004).
16. G. He, X. Wang, A. Zeng, F. Tang, and B. Huang, Chin. Opt. Lett. **5**, 211 (2007).
17. J. Shang, Y. He, D. Liu, H. Zang, and W. Chen, Chin. Opt. Lett. **7**, 732 (2009).
18. M. Philip, K. Morse, and Uno Ingard, *Theoretical Acoustics* (Princeton University Press, 1986).
19. Y. Wang and E.-Z. Fang, J. Nanjing Univ. Sci. Tech. **33**, 69 (2009).
20. L.-S. Zhang, X.-L. Zhang, W.-Y. Tang, and B. Zou, J. Optoelectron. Laser **26**, 103 (2015).